Developmental Cell
Article

Sec1/Munc18 Protein Stabilizes Fusion-Competent Syntaxin for Membrane Fusion in *Arabidopsis* Cytokinesis

Misoon Park,[1] Sonja Touihri,[1] Isabel Müller,[1,3] Ulrike Mayer,[2] and Gerd Jürgens[1,*]
[1]Zentrum für Molekularbiologie der Pflanzen (ZMBP), Entwicklungsgenetik
[2]ZMBP, Mikroskopie
University of Tübingen, Auf der Morgenstelle 3, 72076 Tübingen, Germany
[3]Present address: Regierung von Oberbayern, Technischer Umweltschutz, Gentechnik, 80538, München, Germany
*Correspondence: gerd.juergens@zmbp.uni-tuebingen.de
DOI 10.1016/j.devcel.2012.03.002

SUMMARY

Intracellular membrane fusion requires complexes of syntaxins with other SNARE proteins and regulatory Sec1/Munc18 (SM) proteins. In membrane fusion mediating, e.g., neurotransmitter release or glucose-stimulated insulin secretion in mammals, SM proteins preferentially interact with the inactive closed, rather than the active open, conformation of syntaxin or with the assembled SNARE complex. Other membrane fusion processes such as vacuolar fusion in yeast involve like membranes carrying *cis*-SNARE complexes, and the role of SM protein is unknown. We investigated syntaxin-SM protein interaction in membrane fusion of *Arabidopsis* cytokinesis, which involves cytokinesis-specific syntaxin KNOLLE and SM protein KEULE. KEULE interacted with an open conformation of KNOLLE that complemented both *knolle* and *keule* mutants. This interaction occurred at the cell division plane and required the KNOLLE linker sequence between helix Hc and SNARE domain. Our results suggest that in cytokinesis, SM protein stabilizes the fusion-competent open form of syntaxin, thereby promoting *trans*-SNARE complex formation.

INTRODUCTION

Intracellular membrane fusion requires membrane-anchored SNARE (soluble *N*-ethylmaleimide-sensitive factor attachment receptor) proteins and regulatory Sec1/Munc18 (SM) proteins. When a transport vesicle arrives at a target membrane compartment, a *trans*-SNARE complex forms between v(esicle)-SNARE protein on the vesicle and syntaxin and additional t(arget)-SNARE proteins on the target membrane (Südhof and Rothman, 2009). In addition, SM protein interacts with the cognate syntaxin in its inactive closed, rather than fusion-competent open, conformation or with the assembled SNARE complex by binding to an N-peptide sequence of syntaxin (Dulubova et al., 1999, 2007; Misura et al., 2000; Yamaguchi et al., 2002). Vacuole fusion in yeast represents a different kind of membrane fusion in which like membranes carrying *cis*-SNARE complexes fuse with one another through priming by Sec18p/NSF ATPase followed by *trans*-SNARE complex formation. This process is driven by HOPS complex, which contains the SM protein Vps33p (Wickner, 2010). How Vps33p regulates vacuole fusion is still unknown. In *Arabidopsis*, two of six SM proteins (Sanderfoot et al., 2000) have been functionally related to cognate syntaxins or SNARE complexes. VPS45 positively regulates the SYP41-SYP61-VTI12 SNARE complex in vacuolar trafficking at the TGN/EE (*trans*-Golgi network/early endosomes) (Bassham et al., 2000; Dettmer et al., 2006; Zouhar et al., 2009). SM protein KEULE (KEU) is involved in cytokinesis, interacting with the cytokinesis-specific syntaxin KNOLLE (KN), and also in root-hair development independently of KN (Lukowitz et al., 1996; Lauber et al., 1997; Waizenegger et al., 2000; Assaad et al., 2001). In plant cytokinesis, membrane vesicles derived from the TGN accumulate at the plane of cell division where they fuse with one another to form the cell plate that matures into a new stretch of plasma membrane between the daughter nuclei (Jürgens, 2005). Recently, Touihri et al. (2011) found out that two domains of KN syntaxin—the SNARE domain and the adjacent linker sequence—are essential for membrane fusion in cytokinesis. Here we report that KN-KEU interaction requires the linker sequence, occurs at the cell division plane and involves the fusion-competent open conformation of KN. Our results suggest a model of SM protein action in *Arabidopsis* cytokinesis that is different from SM protein action in other membrane fusion events in that SM protein stabilizes the fusion-competent open form of syntaxin, thereby promoting *trans*-SNARE complex formation.

RESULTS

Mode of Interaction between KN and KEU

The mode of KN-KEU interaction was studied in quantitative yeast two-hybrid assays (Figure 1; Figures S1A and S1B available online). Unexpectedly, KEU interacted with KN only slightly more strongly than with PEP12/SYP21, a PVC/MVB (prevacuolar compartment/multivesicular body)-localized syntaxin (Figures 1A, 1T, and 1U) (Sanderfoot et al., 1998). PEP12 does not complement a *KN* null mutant ($kn^{X37\text{-}2}$) (Müller et al., 2003), and its interaction with KEU was equivalent to the empty-vector

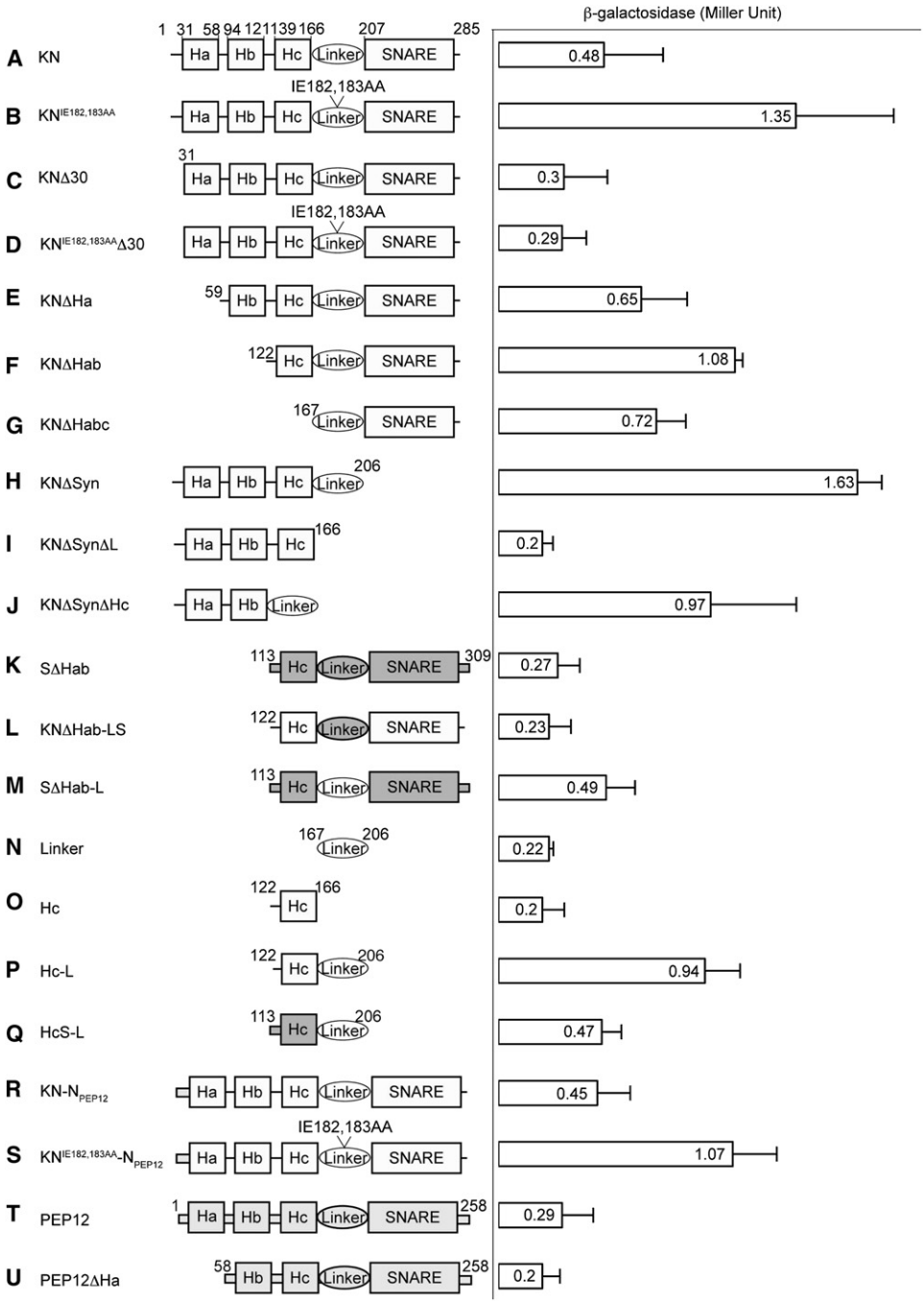

Figure 1. The KN Linker Sequence Is Indispensable for KEU Binding

Diagrams of AD-syntaxin constructs and their quantitative β-galactosidase interaction analysis in yeast coexpressing BD-KEU.

(A) KN, cytosolic fragment without tail anchor.

(B) KN^{IE182,183AA}, KN with IE182,183AA substitution mutations.

(C) KNΔ30, KN lacking N-peptide.

(D) KN^{IE182,183AA}Δ30, KN^{IE182,183AA} without N-peptide.

(E) KNΔHa, KN without N-peptide and helix Ha.

(F) KNΔHab, KN without N-peptide and helices Ha, Hb.

(G) KNΔHabc, KN without entire N terminus.

(H) KNΔSyn, KN without SNARE domain.

(I) KNΔSynΔL, KN with neither SNARE nor linker domain.

(J) KNΔSynΔHc, KN without SNARE domain and helix Hc.

(K) SΔHab, SYP31 without N-peptide and helices Ha, Hb.

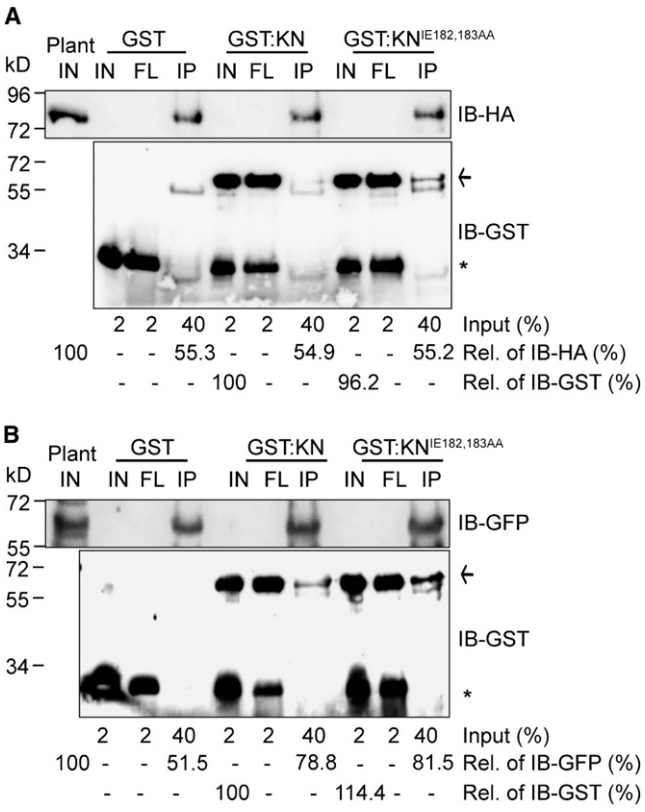

Figure 2. KN Directly Interacts with KEU

Pull-down assays. Purified recombinant GST, GST:KN and GST:KN^{IE182,183AA} proteins (lacking the C-terminal membrane anchor) were tested for interaction with agarose beads-trapped 6×HA:KEU (A) or GFP:SNAP33 (B) isolated from plant extracts. Input (IN), flow-through (FL), and precipitate (IP) were subjected to immunoblot (IB) analysis with antibodies against HA, GFP, or GST. Note that GST:KN^{IE182,183AA} interacts more strongly than GST:KN with both 6×HA:KEU and GFP:SNAP33 (arrows). Asterisks, free GST; kDa (kilodalton), molecular weight markers (left); Input (%), loading volumes relative to the input; Rel. of IB, relative signal intensity (plant input signal = 100% for IB-HA and IB-GFP; input signal of GST:KN = 100% for IB-GST).

See also Figure S2.

control (not shown). Syntaxins adopt two alternative conformations: a closed conformation in which the three N-terminal helices (Habc domain) fold back onto the SNARE domain, forming a four-helical bundle, and an open conformation in which the two regions are physically apart (Margittai et al., 2003b; Sutton et al., 1998). The open form of syntaxin can be experimentally stabilized by two point mutations in the linker between helix Hc and the SNARE domain (Dulubova et al., 1999; D'Andrea-Merrins et al., 2007). Homologous substitutions introduced into KN (KN^{IE182,183AA}) increased the interaction with KEU ~3-fold (Figure 1B), which correlated with its increased susceptibility to limited trypsin proteolysis, suggestive of a more open structure (Figure S1C). To verify this mode of interaction between KN and KEU by a different approach, we performed modified pull-down assays. GST-fused KN or KN^{IE182,183AA} protein was purified from bacterial cells and then incubated with 6×HA:KEU that had been isolated from plant extracts and trapped on agarose beads. Consistent with the results in yeast interaction analysis, GST:KN interacted only weakly with 6×HA:KEU whereas GST:KN^{IE182,183AA} displayed stronger interaction (Figure 2A). Thus, KEU interacts with KN directly and KEU appears to prefer the open conformation of KN for binding. To determine whether the open conformation of KN is competent to interact with its SNARE partners, we performed comparable pull-down assays of the two recombinant KN variants with GFP:SNAP33 purified from transgenic plants in the same manner as 6×HA:KEU. GST:KN^{IE182,183AA} interacted more strongly than GST:KN with SNAP33, which is a KN-interacting *Arabidopsis* SNAP25 homolog also involved in cytokinesis (Heese et al., 2001) (Figure 2B). Taken together, our results suggest that the open conformation of KN is competent to interact with both its SNARE partner(s) and the SM protein KEU.

The Linker Sequence of KN Is Essential for Binding of KEU

To identify KN region(s) essential for interaction with KEU, successively larger deletions were generated from the N-terminus of KN based on its predicted secondary structure (Figure 1) (Lukowitz et al., 1996). Elimination of amino acids 1–30 had no dramatic effect on KN-KEU interaction (Figure 1C), whereas removal of one or more helices of the Habc domain strongly increased the interaction (Figures 1E–1G). Truncated KN lacking the SNARE domain (KNΔSyn) also showed strong binding to KEU (Figure 1H). Furthermore, this interaction was abolished by removal of the linker (KNΔSynΔL), but not the adjacent helix Hc (KNΔSynΔHc, Figures 1I and 1J), demonstrating the essential role of the linker. The linker between helix Hc and the SNARE domain is highly flexible, presumably allowing for conformational changes of syntaxins (Margittai et al., 2003a). We replaced the KN linker with the unrelated linker of the Golgi-localized Sed5p/syntaxin 5 ortholog SYP31 (Figure S2) (Uemura et al., 2004). Neither truncated SYP31 protein (SΔHab) nor the

(L) KNΔHab-LS, KNΔHab with SYP31 linker domain.
(M) SΔHab-L, SΔHab with KN linker domain.
(N) Linker, linker domain of KN.
(O) Hc, helix Hc of KN.
(P) Hc-L, helix Hc, and linker domain of KN.
(Q) HcS-L, helix Hc of SYP31, and KN linker domain.
(R) KN-N_{PEP12}, KN with N-peptide of PEP12 (amino acids 1–20 of PEP12 replaced amino acids 1–42 of KN).
(S) KN^{IE182,183AA}-N_{PEP12}, KN with IE182,183AA substitution mutations and N-peptide of PEP12.
(T) PEP12, cytosolic fragment without tail anchor.
(U) PEP12ΔHa, PEP12 without N-peptide and helix Ha. Domains of PEP12 and SYP31 are marked by light and dark gray color, respectively. Note that all constructs lack the C-terminal membrane anchor (tail anchor) to allow for nuclear uptake. Amino acid positions are indicated. The measurement was repeated three times. Bars in the graph represent SD (n = 12).

See also Figures S1 and S2.

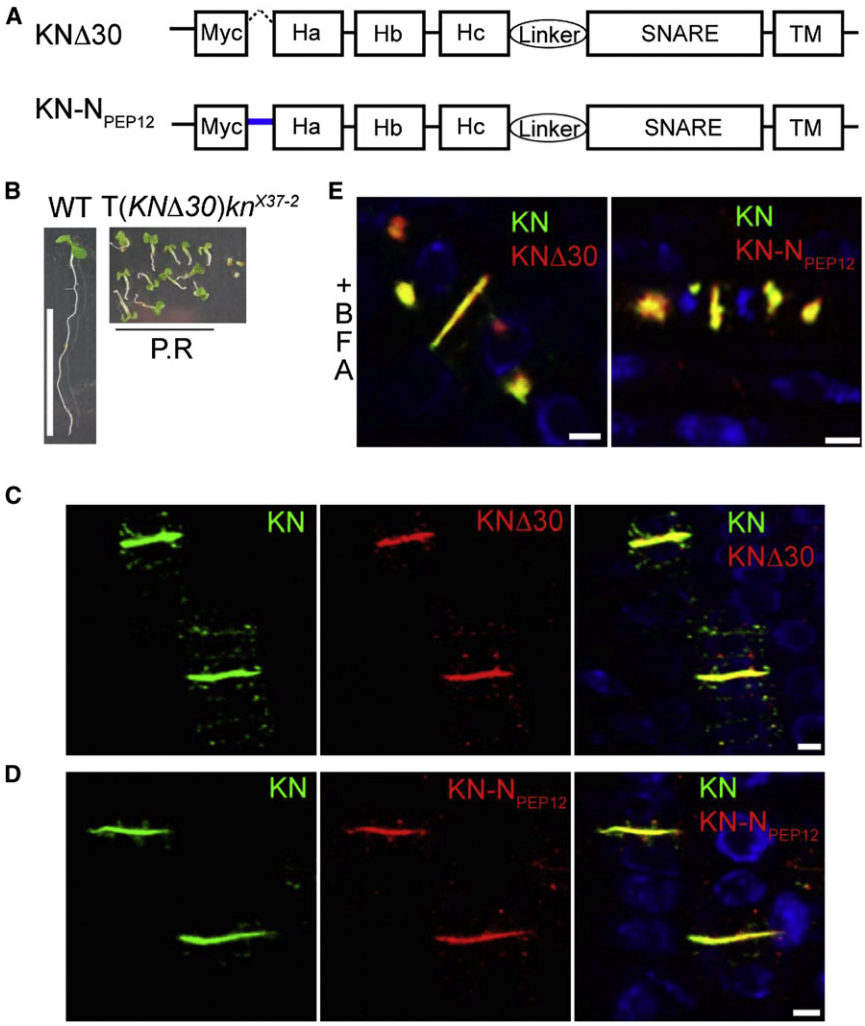

Figure 3. N-Peptide of KN Is Not Sequence-Specifically Required for KEU Binding

(A) Diagrams of KNΔ30 and KN-N_{PEP12}. KNΔ30, KN without N-peptide (amino acids 1–30 deleted); KN-N_{PEP12}, KN with N-peptide of PEP12 (blue line; amino acids 1–42 of KN were replaced with amino acids 1–20 of PEP12). Myc, myc tag; TM, tail anchor.

(B) Complementation analysis. kn^{X37-2} mutant seedlings partially rescued (P.R) by KNΔ30 (right); WT, wild-type. See also Figure S3 for quantitative analysis of complementation test: Note that in contrast to KNΔ30, KN-N_{PEP12} rescues kn^{X37-2} mutant fully.

(C–E) Confocal images of KNΔ30 and KN-N_{PEP12} localization in seedling root cells. Both anti-KN (green) and anti-myc (red) antibodies were used to detect endogenous KN and the engineered versions. Note that anti-KN antiserum recognizes the engineered versions as well because anti-KN antiserum was raised against the entire cytosolic segment of KN (Lauber et al., 1997). (E) Upon 100 μM BFA application, seedlings were immunostained with both anti-myc (red) and anti-KN (green) antibodies. Scale bars represent 1 cm in (B); 5 μm in (C–E).

See also Figure S2.

corresponding KN fragment with the linker from SYP31 (KNΔHab-LS) interacted with KEU (Figures 1K and 1L), suggesting that the KN linker is a sequence-specific binding site for KEU. Unexpectedly, the reciprocal chimera, SΔHab-L displayed slightly enhanced interaction for KEU compared to SΔHab or KNΔHab-LS, but did not interact more strongly than KNΔHab (cf. Figures 1M and 1F), indicating that the molecular context may also play a role in the interaction with KEU. Neither linker nor adjacent helix Hc alone was sufficient for interaction; however, Hc-L comprising both domains was competent to interact with KEU (Figures 1N–1P), implying the necessity of an adjacent domain for the tight interaction with KEU (see also Figure 1G). Interestingly, even the helix Hc from SYP31 (Hc_S-L, Figure 1Q) slightly enhanced the interaction of the KN linker with KEU.

Divergent and Convergent Contribution of N-Peptide to Membrane Fusion

In mammalian membrane fusion mediating (e.g., neurotransmitter release or glucose-stimulated insulin secretion) the N-peptide of syntaxins Syntaxin 1A or Syntaxin 4 is a primary sequence-specific binding site for SM proteins Munc18-1 or Munc18c, respectively, initiating SNARE complex formation (Yamaguchi et al., 2002; Hu et al., 2007; Burkhardt et al., 2008; Rathore et al., 2010). Similarly, the N-peptide of $KN^{IE182,183AA}$ was also required for interaction with KEU in the yeast assay (Figure 1D, $KN^{IE182,183AA}$Δ30). Consistently, KNΔ30 rescued the kn^{X37-2} mutant only partially (Figures 3B and S3), although this protein reached the cell division plane, like KN (Figures 3C and 3E) (Lauber et al., 1997; Reichardt et al., 2007). Thus, the N-peptide is important for KN functionality. Interestingly, however, alanine substitutions of the conserved amino acid residues T6 and F9, which correspond to the essential residues of yeast syntaxins Sed5p and Ufe1p in the SM protein Sly1p-binding pocket (Bracher and Weissenhorn, 2002; Yamaguchi et al., 2002), did not disrupt KN function (data not shown). Furthermore, a chimeric KN protein containing the sequence-unrelated N-peptide of PEP12 (Figure S2) was able to substitute functionally for wild-type KN (Figures 3A, 3D, 3E, and S3B). Indeed, $KN^{IE182,183AA}$-N_{PEP12} interacted strongly with KEU in yeast analysis, unlike KN-N_{PEP12}, which was reminiscent of the difference in interaction with KEU between $KN^{IE182,183AA}$ and wild-type KN (Figures 1R and 1S, cf. Figures 1A and 1B). Taken together, these results suggest that the KN-KEU interaction requires the presence, but not a specific sequence, of an N-peptide, in contrast to sequence-specific requirement of the KN linker.

KN Without the Genuine Linker Sequence Is Not Functional In Vivo

To determine the biological significance of the KN linker, we generated transgenic plants expressing, from *KN cis*-regulatory

sequences (Müller et al., 2003), three KN variants fused to either vYFP (Nagai et al., 2002) or myc (Müller et al., 2003) at their N terminus: KN without linker (KNΔL), KN with the linker of SYP31 in place of its own (KN-LS), and KN with two point mutations in the linker ($KN^{IE182,183AA}$), corresponding to a constitutively open form (Figure 4A). Transgenic plants expressing GFP:KN were used as control (Reichardt et al., 2007). All three mutant fusion proteins had the expected sizes (Figure S4A) and were indistinguishable in their subcellular localization and dynamics from the wild-type form of KN (Figures 4B, 4C, and S4B). Consistent with the data of the yeast analysis, both KNΔL and KN-LS, which lacked the genuine KN linker, failed to rescue the kn^{X37-2} mutant (Figures 4D, S4C, S4D, and S4G). In contrast, $KN^{IE182,183AA}$ rescued the kn^{X37-2} mutant, depending on the amount of protein made (Figures 4D and S4E–S4G). This result suggests that $KN^{IE182,183AA}$ actually resembles the active form of KN, consistent with the result of the pull-down assay in which $KN^{IE182,183AA}$ strongly interacted with SNAP33 (Figure 2B). Thus, the linker between N-terminal helices and SNARE domain is not necessary for KN trafficking but is absolutely essential for KN function at the cell plate, by acting as a sequence-specific binding site for KEU.

Overexpression of the Open Conformation of KN Bypasses the Necessity of KEU

To explore the biochemical interaction of KN and its variants with KEU in planta, immunoprecipitation was performed with extracts from transgenic plants that coexpressed 6×HA:KEU and each myc-tagged KN variant (Figure 4E). Myc-KN was coimmmunoprecipitated with KEU, although only a small amount of KN was detected in the KEU-bound fraction. A similar observation has been made on the interaction of neuronal syntaxin 1 with SM protein Munc18-1 (Gerber et al., 2008). In contrast to KN, neither KNΔL nor KN-LS were bound to KEU (Figure 4E). These results suggest that the linker of KN is a sequence-specific binding site for KEU. Surprisingly, $KN^{IE182,183AA}$ was undetectable in the KEU-precipitated fraction, although the two proteins interacted strongly in the yeast interaction and pull-down assays (Figure 4E; see also Figures 1B and 2A). Interestingly, however, $KN^{IE182,183AA}$ displayed an enhanced interaction with the SNARE partner of KN, SNAP33, apparently at the expense of KN-KEU interaction (Figure 5A, cf. Figure 4E). These results raised the possibility that KN might interact with its SNARE partners or with KEU but not with both at the same time. We addressed this problem by coimmunoprecipitation of extracts from plants expressing differentially tagged KEU, SNAP33, and either KN or $KN^{IE182,183AA}$. KEU did not coimmunoprecipitate SNAP33 but did interact with KN, suggesting that KEU does not interact with the assembled KN-containing SNARE complex (Figure 5B). However, there was no interaction of KEU with the open conformation of KN, as observed before (see Figure 4E). In the reciprocal experiment, SNAP33 also did not coimmunoprecipitate KEU, thus confirming the result (Figure S5D). Interestingly, however, in this case, SNAP33 interacted more strongly with the open conformation than with the normal form of KN, as already observed (Figure S5D, see also Figure 5A). Taken together, our results strongly suggest that KEU interacts with monomeric KN preferentially in its open conformation rather than the assembled SNARE complex. However, we cannot completely rule out the possibility that there is residual interaction of KEU with the assembled SNARE complex that escapes detection for technical reasons. Because KEU preferentially interacts with the open conformation of monomeric KN, which appears to be a transitory state of syntaxin from the closed monomer to the assembled complex, we analyzed whether a constitutively open conformation of KN might bypass the requirement of KEU in cytokinesis. As shown in Figures 5C and S5A–S5C, $KN^{IE182,183AA}$ was able to suppress a *KEU* null mutant phenotype (keu^{MM125}). Thus, the constitutively open conformation of KN appears to form the *trans*-SNARE complex without requiring KEU activity in cell-plate formation.

KN Interacts with KEU at the Cell Division Plane

The keu^{MM125} mutant was also rescued by KEU with an N-terminal 6×HA tag expressed from the *KN cis*-regulatory sequences (Figures S6A–S6C), which displayed a punctate pattern, with stronger signals at the plane of cell division (Figure 6A). Surprisingly, KEU localization was insensitive to the ARF-GEF inhibitor brefeldin A (BFA) (Figures 6B and S6G) (Geldner et al., 2003), and KEU did not colocalize with the Golgi/TGN marker ARF1 (Figure S6E) (Stierhof and El Kasmi, 2010), suggesting that KEU, unlike KN, is not trafficked to the plane of cell division through the TGN. Whereas neuronal SM protein Munc18-1 escorts syntaxin 1A to the plasma membrane (Liu et al., 2004), KN reaches the cell plate in a KEU-independent manner (Waizenegger et al., 2000). Likewise, KEU did not require KN for reaching the plane of cell division (Figures 6C and 6D). These data suggest that KN interacts with KEU only at the division plane where this interaction might promote the formation of the *trans*-SNARE complex.

Interaction of KN with KEU Is a Pivotal Step in Plant Cytokinesis

As shown in Figure 1P, the KN fragment comprising the Hc helix and the linker (Hc-L) interacted strongly with KEU. To analyze whether Hc-L overexpression interferes with KN function by titrating out KEU, we generated transgenic plants expressing vYFP-labeled Hc-L fusion protein either conditionally using the GAL4>>UAS two-component system (Weijers et al., 2003) or from the *KN cis*-regulatory sequences (Figures 7A and S7A). Activation of Hc-L expression caused a growth-retarded seedling phenotype of short and thickened root compared to wild-type (Figure 7B; see also Figure S7B), with disorganized cell shapes and cell-wall stubs suggesting cytokinesis defects (Figures 7C, 7D, and S7C). These defects were less severe than those in kn^{X37-2} or keu^{MM125} single mutants, possibly because Hc-L bound KEU less efficiently than did a constitutively open form of KN (Figures 1B and 1P).

Fusion protein vYFP:Hc-L was detected in the cytosol and, interestingly, at the plane of cell division as shown by colabeling of the associated phragmoplast, a microtubule array assisting in cell-plate formation (Figure 7E, inset). Because KN protein lacking the C-terminal membrane anchor is entirely cytosolic (Völker et al., 2001) and Hc-L protein was BFA-insensitive (Figure S7D), unlike KN, KEU interaction might mediate Hc-L localization to the cell division plane. Whereas wild-type embryos displayed Hc-L at the cell division plane as did the root cells, Hc-L was redistributed to the cytosol in the multinucleated cells of keu^{MM125} mutant

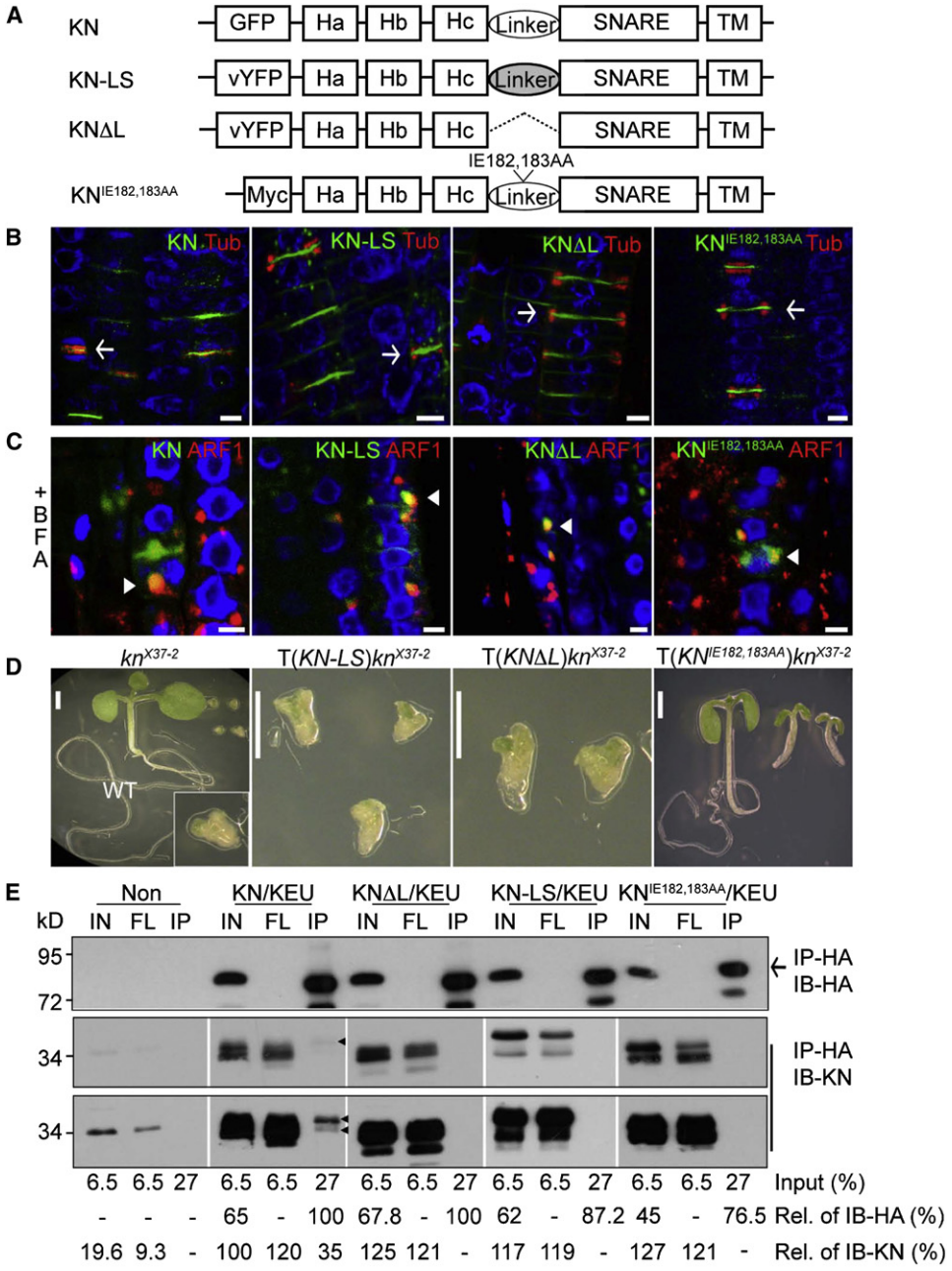

Figure 4. The Linker Sequence Is Essential for KN Function

(A) Domain structures of constructs; KN-LS, KN with SYP31 linker (gray); KNΔL, KN without linker; KN^{IE182,183AA}, constitutively open conformation of KN. GFP, vYFP, Myc, epitopes; TM, tail anchor.

(B and C) Confocal images of seedling root cells stained for KN derivatives (green) and tubulin (B, red) or ARF1 after 100 μM BFA treatment (C, red), and counterstained with DAPI (blue). Note that KN^{IE182,183AA} was detected with anti-myc antibody. Arrows, cell plate with phragmoplast (red); arrowheads, BFA compartment with KN and ARF1 signals merged.

(D) Complementation analysis. T2 seedlings harboring indicated transgene (T) in *kn*$^{X37-2}$ homozygous background. Left: WT, wild-type; inset: *kn*$^{X37-2}$ mutant. Note that KN^{IE182,183AA} rescue of *kn*$^{X37-2}$ is dosage-dependent.

(E) Coimmunoprecipitation analysis. Immunoprecipitation (IP) with anti-HA beads (6×HA:KEU) was followed by immunoblot (IB) analysis. The middle and bottom panels show immunoblots exposed for 0.5 min and 3–4 min, respectively. kDa, (kilodalton), molecular weight markers (left); Input (%), loading volumes relative to the input. Rel. of IB, relative signal intensity: IP signal (KN/KEU) = 100% for IB-HA; input signal (KN/KEU) = 100% for IB-KN. Arrow, 6×HA:KEU; arrowheads, myc:KN. Note the detection of myc:KN protein as doublet (Lauber et al., 1997) and no coimmunoprecipitation of endogenous KN with KEU due to the low protein level. Non, nontransformed plant; IN, input; FL, flow-through. Scale bars represent 5 μm in (B) and (C); 1 mm in (D).

See also Figures S2 and S4.

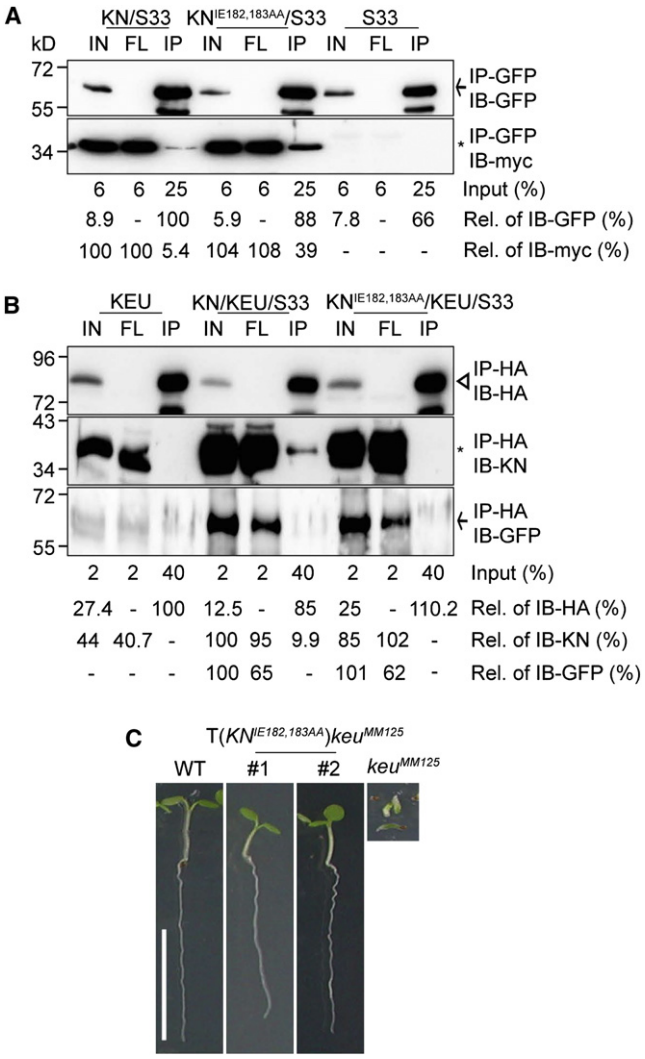

Figure 5. The Constitutively Open Conformation of KN Does Not Require KEU Activity

(A and B) Coimmunoprecipitation analyses. (A) Immunoprecipitation (IP) with anti-GFP beads (S33, GFP:SNAP33) from transgenic plants coexpressing GFP:SNAP33 and myc:KN or myc:KN^{IE182,183AA} was followed by immunoblot (IB) analysis. (B) Immunoprecipitation (IP) with anti-HA beads (6×HA:KEU) from transgenic plants coexpressing 6×HA:KEU, GFP:SNAP33 and either myc:KN or myc:KN^{IE182,183AA} was followed by immunoblot (IB) analysis. See also Figure S5D for the reciprocal coimmunoprecipitation experiment with anti-GFP beads (GFP:SNAP33). kDa (kilodalton), molecular weight markers (left); Input (%), loading volumes relative to the input. Arrows, GFP:SNAP33; asterisks, myc:KN or myc:KN^{IE182,183AA}; triangle, 6×HA:KEU. IN, input; FL, flow-through; Rel. of IB, relative signal intensity: IP signal (KN/S33) = 100% for IB-GFP in (A); input signal (KN/S33) = 100% for IB-myc in (A); IP signal (KEU) = 100% for IB-HA in (B); input signal (KN/KEU/S33) = 100% for IB-KN and IB-GFP in (B).

(C) Seedlings harboring myc-tagged *KN*^{IE182,183AA} transgene (T) in *keu*^{MM125} homozygous background. WT, wild-type; *keu*^{MM125}, nontransformed mutant. Scale bar represents 1 cm in (C).

See also Figure S5.

embryos (Figures 7E–7G and S7E). In conclusion, the linker separating the N-terminal Habc domain from the SNARE domain of KN is an essential site for KN-KEU interaction at the division plane, which, in turn, is a pivotal regulatory step for membrane fusion during cytokinesis in *Arabidopsis*.

DISCUSSION

In eukaryotes, there are two types of membrane fusion: heterotypic fusion, which occurs between a transport vesicle and its target membrane, and homotypic fusion, which occurs between two biochemically identical membranes such as yeast vacuoles and mammalian endosomes. Both types of fusion are mediated by a core fusion machinery comprising interacting SNARE proteins and regulatory SM proteins. In heterotypic membrane fusion, such as neurotransmitter release or glucose-stimulated insulin secretion, SM proteins Munc18-1 or Munc18c interact with the closed conformation of its cognate syntaxin by binding the N-peptide of the syntaxins Syntaxin 1 or Syntaxin 4, respectively. This specific interaction appears to initiate SNARE complex formation and extends to the open syntaxin in the assembled SNARE complex, thus facilitating subsequent membrane fusion (Rathore et al., 2010), although this working model is still controversial (Burkhardt et al., 2008). Maintaining the closed conformation of syntaxin prior to fusion of the vesicle with its target membrane is very important for gating the initiation of membrane fusion in neurotransmitter release (Gerber et al., 2008). This is consistent with the notion that syntaxin kept inactive (closed) during transport switches to an active (open) form just before membrane fusion to prevent ectopic SNARE complex formation and thus promote specificity of membrane fusion. How, then, is the switch from a closed to an open conformation of syntaxin regulated? Recently, Munc13-1 involved in neurotransmitter release has been demonstrated to promote the transition of the closed to the open conformation of syntaxin 1 via weak protein-protein interaction with the SNARE domain at the presynaptic active zone (Ma et al., 2011). This result explains the previous observation that the overexpression of the open conformation of syntaxin completely rescues the *unc13* mutant phenotype in *Caenorhabditis elegans* (Hammarlund et al., 2007). Thus, transition of syntaxin from closed to open conformation appears to be one major regulatory steps in heterotypic membrane fusion. In contrast to the action of SM proteins in heterotypic fusion processes, the role of SM protein in homotypic membrane fusion has not been well defined, although yeast vacuolar fusion and mammalian endosomal fusion have been studied in some detail (reviewed in Carr and Rizo, 2010).

Although the issue of whether the cell plate in plants is mainly formed through homotypic or heterotypic vesicle fusion events remains unresolved, several lines of evidence suggest that the cell plate in plants is mainly formed by fusion events that involve a uniform population of membrane vesicles derived from Golgi/TGN and might thus be regarded as homotypic membrane fusion. This evidence includes: (1) morphologically identical membrane vesicles ~60 nm in diameter are aligned properly in the plane of cell division in *knolle* or *keule* mutants but fail to fuse with one another (Waizenegger et al., 2000); (2) inhibition of the secretory, but not the endocytic, pathway entails cytokinesis defects (Reichardt et al., 2007); (3) KN is newly synthesized during mitosis (Lauber et al., 1997), delivered to the plane of cell division, not to the plasma membrane, via the secretory pathway and degraded in the vacuole shortly after cytokinesis (Reichardt

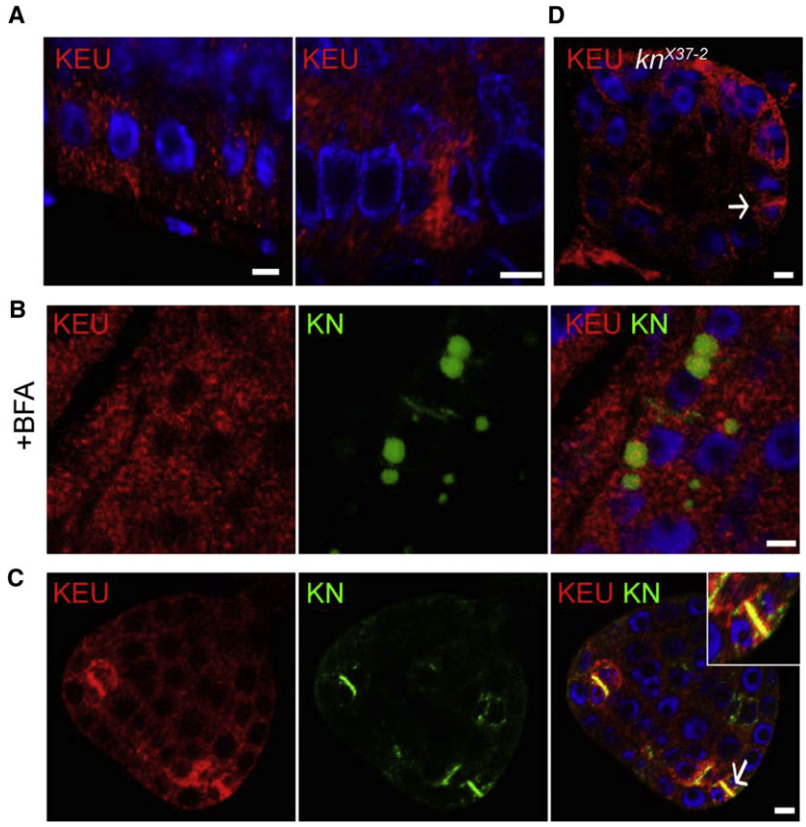

Figure 6. KN Interacts with KEU at the Cell Division Plane

Confocal images of seedlings (A and B) and embryos (C and D) expressing 6×HA:KEU and labeled with anti-HA antibody (red) or anti-KN antiserum (green) and counterstained with DAPI (blue). (A) KEU displays ubiquitously distributed punctate signals in most root cells (left) and stronger signals at the cell division plane (right). (B) In contrast to KN (green), KEU does not accumulate in BFA compartments. (C) Wild-type embryo; (D) *kn*$^{X37-2}$ homozygous embryo. Arrows (C and D), cell division plane. Scale bar represents 5 μm in (A–D).

See also Figure S6.

et al., 2007, 2011); and (4) KN-related syntaxin SYP132, which is not endocytosed, can rescue the *knolle* mutant only when expressed from the *KN cis*-regulatory sequences (Reichardt et al., 2011). Endocytosis has been proposed to mediate cell plate formation in *Arabidopsis* cytokinesis (Dhonukshe et al., 2006), whereas other evidence suggests that its contribution is locally restricted to the cortical division zone (CDZ) recruitment pathway (Van Damme et al., 2011). Although endocytosis delivers proteins to the forming cell plate, there is no direct evidence for its functional requirement for cell plate formation (Reichardt et al., 2007, 2011). Taken together, secretory traffic of de novo synthesized proteins is far more important to cytokinesis than is endocytosis. If the cell plate is indeed formed by homotypic membrane fusion it would be interesting to determine whether this specific mode of syntaxin-SM protein interaction is unique to plant cytokinesis or whether it might also apply in homotypic membrane fusion processes in other eukaryotes.

Our study of membrane vesicles fusing with one another in plant cytokinesis revealed that SM protein KEU binds the open conformation of monomeric syntaxin KN but neither its closed form nor the assembled SNARE complex, although we cannot completely rule out the possibility of residual interaction of KEU with the assembled SNARE complex. These results suggest the following model of KN-KEU interaction in cytokinesis (Figures 7H–7N). TGN-derived membrane vesicles carry *cis*-SNARE complexes in which syntaxin KN is paired with its SNARE partners. Upon arrival at the plane of cell division, the *cis*-SNARE complexes are broken up by NSF ATPase, and resident SM protein KEU binds to the open form of KN to prevent its folding into the inactive closed form. The open form of KN thus stabilized is competent to form *trans*-SNARE complexes with SNARE partners residing on adjacent vesicles, promoting membrane fusion that results in the formation of the partitioning membrane between the daughter nuclei of the dividing cell. In this scenario, membrane fusion in plant cytokinesis would differ from heterotypic membrane fusion between vesicles and their target membrane not only in the occurrence of *cis*-SNARE complexes before, rather than after, membrane fusion but also in the interaction between SM protein and the open, rather than the closed, form of syntaxin. Although the interaction between SM protein and the open conformation of syntaxin is well supported by our results, it is not known when and where *cis*-SNARE complexes of KN are formed prior to their interaction with KEU.

Deletion of the N-peptide of KN disrupts KN function in vivo, suggesting that the N-peptide is necessary for KN function through its interaction with SM protein KEU, like it is in heterotypic membrane fusion (reviewed in Südhof and Rothman, 2009). However, an unrelated N-peptide of PEP12 can completely replace the function of the N-peptide of KN, assisting in linker-mediated interaction with KEU and in KN function. Thus, the N-peptide of syntaxin is not a sequence-specific binding site for SM protein in membrane fusion during plant cytokinesis but rather might play an auxiliary role in the interaction between syntaxin and SM protein. In contrast to the N-peptide, the linker adjacent to the SNARE domain of KN is a sequence-specific binding site for KEU. By binding to the linker, KEU prevents the transition of the open to the closed form of KN. However, the linker sequence in itself is not sufficient to interact with the SM protein but requires adjacent domains such as helix Hc or SNARE domain for stabilization.

The linker sequence of syntaxin KN is a sequence-specific and essential binding site for SM protein KEU. However, there is some evidence for this kind of interaction in other membrane fusions as well. For example, Munc18c and Syntaxin 4 involved in glucose-stimulated insulin secretion interact not only via the N-peptide but also, at least in vitro, via syntaxin residues 118–194 corresponding to Hc helix and linker sequence of KN

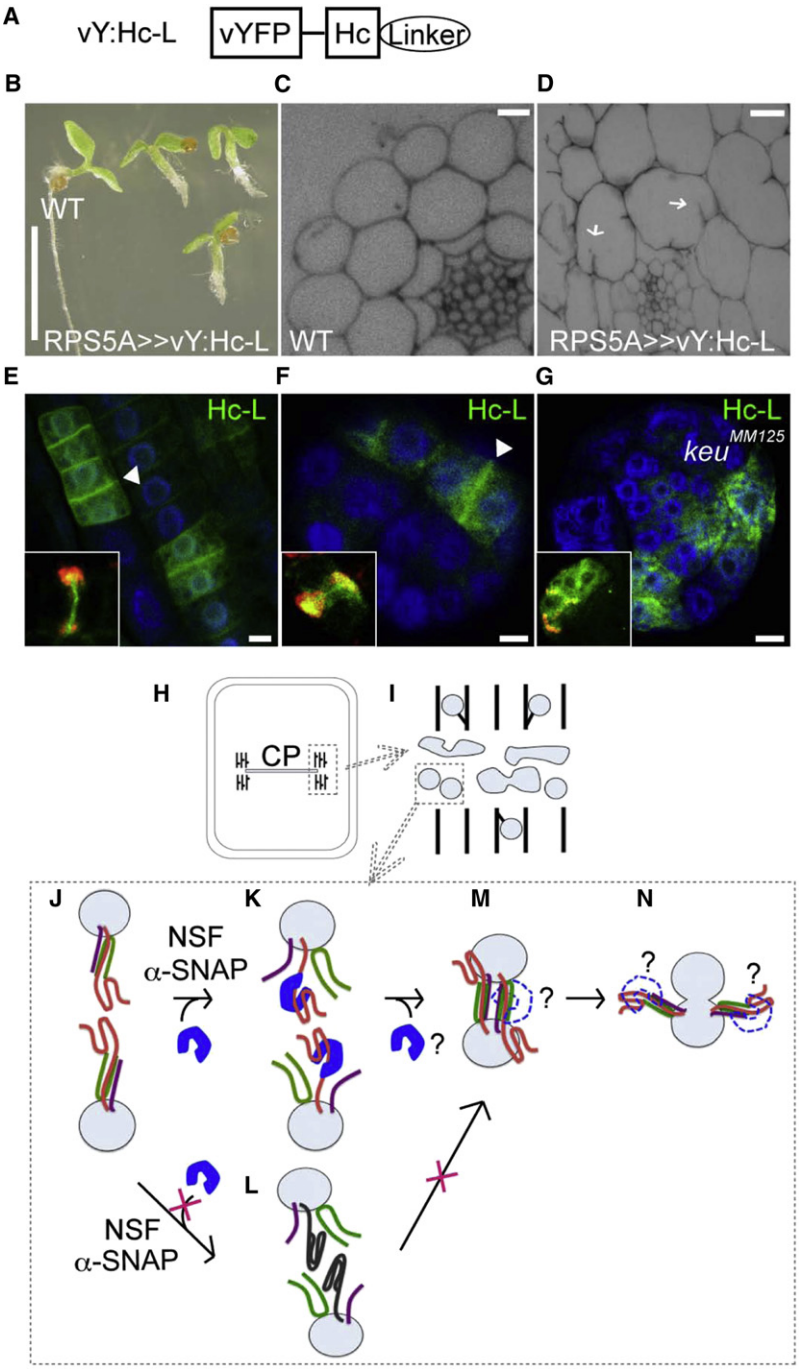

Figure 7. KN-KEU Interaction Promotes Membrane Fusion in Cytokinesis

(A–G) Functional analysis of KEU-interacting KN fragment including the linker. (A) Domain structure of vYFP:Hc-L. (B–D) F1 progeny of RPS5A>>vYFP:Hc-L (B) stocky seedlings; WT, wild-type; (C and D) root cross-sections displaying cell-wall stubs (D, arrows). (E–G) Confocal images of seedling root (E), wild-type (F), and *keu*^{MM125} (G) embryos expressing KN::vYFP:Hc-L (green) and counterstained with DAPI (blue). Arrowheads (E and F) indicate cell plates; insets show cell plates labeled with vYFP:Hc-L (green) and associated phragmoplasts counterstained with anti-tubulin antibody (red; see also Figure S7E). Note absence of cell plate-positive signals in *keu*^{MM125} embryo (G), only the phragmoplast signal (red) remains (G, inset). Scale bars represent 1 cm (B); 12 μm (C and D); 5 μm (E–G).

(H–N) Model of KN-KEU interaction in membrane fusion during cytokinesis. (H) Cell plate (CP) formation. (I) Delivery of TGN-derived vesicles to the division plane along phragmoplast microtubules. (J–N) *trans*-SNARE complex formation: (J) *cis*-SNARE complexes are broken up by NSF and α-SNAP, (K) KEU (blue) binds to the open, fusion-competent, form of KN (red), (L) to prevent its refolding into the closed form (black), (M) followed by KN complex formation with SNARE partners (SNAP33, green; VAMP, purple) residing on adjacent vesicles. (N) Membrane fusion resulting in *cis*-SNARE complexes. Note that KEU interacts with the monomeric open form of KN and might be released after *trans*-SNARE complex formation. However, continued interaction of KEU with the assembled SNARE complex cannot be excluded (KEU, dashed blue, in M and N). This illustration was adapted from Misura et al. (2000) and Jürgens (2005).

depending on the phosphorylation status of the Y219 residue of Munc18c (Jewell et al., 2008). Another case might be Munc18-1 and Syntaxin 1A involved in neurotransmitter release. Munc18-1 interacts not merely with full-length Syntaxin 1A via the N-peptide but also with N-terminally truncated Syntaxin 1A lacking the N-peptide and the three helices Habc, which is sufficient to stimulate membrane fusion in a single-vesicle fusion assay (Diao et al., 2010). These results raise the possibility that the syntaxin linker is somehow involved in syntaxin-SM protein interaction in other kinds of membrane fusion, although its functional relevance remains elusive, unlike the essential and sequence-specific role of the N-peptide of the closed monomeric syntaxin in initiating binding of the SM protein. In contrast, membrane fusion in *Arabidopsis* cytokinesis requires binding of the SM protein to the linker sequence of the open monomeric syntaxin in a sequence-specific manner.

In conclusion, our results reveal that in *Arabidopsis* cytokinesis, syntaxin interacts in its open conformation through its linker adjacent to the SNARE domain with the cognate SM protein and that this sequence-specific interaction is a crucial step in membrane fusion. It remains to be determined whether this mode of interaction is unique to plant cytokinesis or occurs in other eukaryotic membrane fusion processes as well.

EXPERIMENTAL PROCEDURES

Molecular Biology

See Supplemental Experimental Procedures.

Yeast Analysis

The EGY48 yeast strain was transformed with three plasmids—lacZ reporter pSH18-34, pEG202::KEU, and an individual pJG4-5::KN variant—using

a polyethylene glycol (PEG) transformation method (33.3% [w/v] PEG3500, 100 mM LiAc, 0.3 mg/ml ssDNA). Quantitative β-galactosidase analysis was performed as follows. In brief, cell mass was suspended in reaction solution (buffer H [100 mM HEPES pH 7, 150 mM NaCl, 2 mM $MgCl_2$, 1% [w/v] BSA], 6.1% [v/v] chloroform, 0.006% [w/v] SDS) followed by addition of ortho-nitrophenyl-β-galactoside (ONPG, 4 mg/ml in buffer H, Sigma-Aldrich). The Miller Units of each sample were calculated [(1,000 × OD_{420})/(culture volume × time × OD_{600})] (Miller, 1972). Each measurement was done with four independent colonies and repeated three times.

Trypsin Treatment

T7-tagged KN and $KN^{IE182,183AA}$ proteins were purified from BL21(DE3)pLys bacterial cells, using anti-T7-beads (Merck-Novagen) according to the manufacturer's instructions, suspended in cold PBS, immediately followed by the addition of trypsin (1 M stock solution in PBS; always freshly prepared, Sigma-Aldrich). The reaction was stopped by addition of 1× Laemmli buffer and boiling for 5 min at the 95°C.

Plant Material, Growth Condition, and Transformation

Arabidopsis thaliana wild-type—Columbia (Col-0) or Landsberg (Ler)—plants were grown on soil at 18°C or 23°C in long-day conditions (Mayer et al., 1991). Wild-type or heterozygous plants either of kn^{X37-2} or of keu^{MM125} were transformed with *Agrobacterium tumefaciens*, using the floral-dip method (Clough and Bent, 1998). *KN::myc:KN* (Müller et al., 2003) or *KN::GFP:KN* (Reichardt et al., 2007) plants were crossed with *KN::6×HA:KEU* plants for the coimmunoprecipitation or immunofluorescence analyses. *RPS5A::GAL4* (Weijers et al., 2003) plants were crossed with T1 plants of *UAS::vYFP:Hc-L* for phenotypic analysis. *35S* (Cauliflower Mosaic Virus promoter)*::GFP:SNAP33* line was provided by Dr. Liliane Stricher and crossed with the transgenic plants bearing *myc:KN*, $myc:KN^{IE182,183AA}$ or *KN::6×HA:KEU* for the coimmunoprecipitation experiment.

Genetic Analysis

T1 plants grown on soil from bulk-harvested seeds were selected for transformants by spraying three times with a 1:1,000 diluted BASTA (183 g/l glufosinate; AgrEvo, Düsseldorf, Germany). Selected BASTA-resistant plants were genotyped. PCR-genotyping: kn^{X37-2}, primers X37-2CIII and X37-2DIII, which amplify a 0.5-kb fragment from kn^{X37-2} and a 1.5-kb fragment from wild-type KN (Müller et al., 2003); keu^{MM125}, primers KEU in 14 and KEU in 17 giving a 0.4-kb fragment from keu^{MM125} and a 0.5-kb fragment of wild-type *KEU*; *vYFP:KN-LS* or *vYFP:KNΔL*, primers $vYFP_{forward}$ and $KN_{reverse}$ giving an ~1-kb fragment of each transgene; $myc:KN^{IE182,183AA}$, *myc:KNΔ30*, or *myc:KN-*N_{PEP12}, primers $myc_{forward}$ and $KN_{reverse}$ giving an ~1-kb fragment of each transgene; *6×HA:KEU*, primers $HA_{forward}$ and KEU400 giving an ~0.6-kb fragment. Genomic DNA was isolated using a cetyltrimethylammonium bromide (CTAB)-based miniscale protocol as previously reported (Assaad et al., 2001). For seedling observation, seeds were germinated on solid medium (2.15 g/l MS salts, 1 g/l MES, 1% [w/v] sucrose, pH 5.6) in the same growth condition as described above. Segregation of antibiotics resistance was counted on phosphinothricin (PPT, 15 mg/l)-supplemented medium.

Coimmunoprecipitation

Five grams of inflorescence or 5-day-old seedlings was ground thoroughly in liquid nitrogen and suspended in lysis buffer (50 mM Tris pH 7.5, 150 mM NaCl, 0.5% [v/v] Triton X-100) supplemented with an EDTA-free protease inhibitors cocktail (Roche Diagnostics). After 30 min incubation on ice, cell debris-removed supernatants were incubated with anti-HA (Sigma-Aldrich) or anti-GFP (GFP-trap, Chromotek) beads for 2 hr in the cold room with mild rotation. The beads were rinsed four times with washing buffer (50 mM Tris pH 7.5, 200 mM NaCl [for the interaction analysis of KN variants/GFP:SNAP33, 150 mM NaCl was used instead], 0.2% Triton X-100) supplemented with EDTA-free protease inhibitors cocktail, and resuspended in washing buffer and Laemmli buffer.

Pull-Down Assay

HA-tagged KEULE (6×HA:KEU) or GFP-tagged SNAP33 (GFP:SNAP33) was purified using anti-HA or anti-GFP beads as described in coimmunoprecipitation method. GST, GST:KN, and $GST:KN^{IE182,183AA}$ proteins were purified from BL21(DE3)pLys bacterial cells, using anti-GST-beads and 10 mM reduced L-glutathione (Sigma-Aldrich) according to the manufacturer's instructions. Equal amount of eluted GST variants was incubated with agarose beads-trapped 6×HA:KEULE or GFP:SNAP33 in the cold room with mild rotation in buffer (50 mM HEPES 7.5; 150 mM NaCl; 1 mM $MgCl_2$; 1 mM EDTA; 0.5% Triton X-100) supplemented with protease inhibitors cocktail. After overnight incubation, beads were rinsed five times with washing buffer (50 mM HEPES 7.5; 200 mM NaCl; 1 mM $MgCl_2$; 1 mM EDTA; 0.2% Triton X-100) supplemented with protease inhibitors cocktail and subjected to immunoblot analysis.

Immunoblots and Immunofluorescence Analysis

For immunoblot analysis of proteins from yeast cells, individual yeast transformants were grown overnight. The cell mass was suspended in 1× Laemmli buffer and immediately frozen in liquid nitrogen. After incubation at 95°C for 20 min, supernatants were immuno-analyzed. For detection of BD-fused KEU and AD-fused KN variants, anti-LexA (1:1,000, Santa Cruz Biotechnologies) and POD-conjugated anti-HA antibodies (1:1,000, Roche Diagnostics) were used, respectively.

For immunoblot analysis of proteins from plants, inflorescences from T1 plants or entire T2 seedlings were harvested. Total proteins were extracted with lysis buffer supplemented with an EDTA-free protease inhibitors cocktail. Antibodies of anti-KN (rabbit, 1:5,000) (Lauber et al., 1997), anti-tubulin (mouse, 1:1,000, Sigma-Aldrich), anti-myc 9E10 (mouse, 1:1,000, Santa Cruz), POD-conjugated anti-HA, anti-YFP (rabbit, 1:1,000, a gift from S. de Vries), anti-GFP (rabbit, 1:1,000, Invitrogen), and POD-conjugated anti-GST (rabbit, 1:2,000, Sigma-Aldrich) were used to detect the indicated proteins. POD-conjugated secondary antibodies (1:7,000, Sigma) were used in all immunoblot analyses except for "IP-GFP/IB-myc" shown in Figure S5D, which was detected with alkaline phosphatase (AP)-conjugated secondary antibody (1:7,000, Novagen). Membranes were developed using both conventional method (AGFA film developing system) and a chemiluminescence detection system (Fusion Fx7 Imager, PEQlab, Germany).

Immunostaining of seedling roots was performed as previously reported (Völker et al., 2001). In brief, ~5-day-old seedlings were fixed in 4% (w/v) paraformaldehyde and labeled with the indicated antibodies. For brefeldin A (BFA) treatment, ~5-day-old seedlings were treated with 100 μM brefeldin A (50 mM stock solution in 1:1 DMSO/EtOH, Invitrogen) for 1 hr followed by fixation.

For immunofluorescence, anti-KN (rabbit, 1:2,000), anti-tubulin (rat, 1:1,000, Abcam, Boston), anti-HA (mouse, 1:1,000, BAbCO, Richmond, CA), anti-myc 9E10 (mouse, 1:1,000, Santa Cruz), two sorts of anti-ARF1 (anti-ARF1 for Figures 3C and S4B [rabbit, 1:1,000] [Pimpl et al., 2000]: anti-ARF1 for Figures S6E and S7D [rabbit, 1:1,000, Agrisera]), anti-mouse FITC (1:600, Dianova), anti-rabbit-Cy3™ (1:600, Dianova), and anti-rabbit-Alexa488 (1:600, Invitrogen) were used.

Embryos were prepared as previously reported (Heese et al., 2001). In brief, embryos were fixed in 4% paraformaldehyde plus 1% Triton X-100 and then squeezed out of the seed coat on gelatin-coated slides. Fluorescence images were taken using a confocal laser scanning microscope (Leica) and Leica TCS software.

Phenotypic Analysis

Seedling sectioning was performed as previously reported (Heese et al., 2001). In brief, ~7-day-old seedlings were fixed in 4% paraformaldehyde, dehydrated in a series of ethanol, and embedded in LR-white resin (London Resin). Sections were cut in 3- to 5-μm thick slices using a cryomicrotome (Supercut 2065) and stained with toluidine blue.

Software

Sequences were analyzed using Vector NTI (Invitrogen). Images were processed using Adobe Photoshop CS3 and Adobe illustrator CS3. Quantification of signal intensity in immunoblot analysis was done using ImageJ program (NIH).

SUPPLEMENTAL INFORMATION

Supplemental Information includes seven figures, Supplemental Experimental Procedures, and one table and can be found with this article online at doi:10.1016/j.devcel.2012.03.002.

ACKNOWLEDGMENTS

We thank Ulrike Hiller for technical assistance, Sacco de Vries (Wageningen University, Netherlands) and Liliane Sticher (University of Fribourg, Switzerland) for providing materials, and Martin Bayer, Niko Geldner, Rita Groß-Hardt and our group members for critical reading of the manuscript. This work was funded by the Korea Research Foundation through fellowship C00066 to M.P. and the Deutsche Forschungsgemeinschaft through grant Ju 179/14-1. M.P. performed most of the experiments. S.T. did the genetic study and immunofluorescence analysis of KNΔ30 and 6×HA:KEULE in embryos. I.M. performed the functional study of KN-N_{PEP12} and generated the transgenic plants bearing *KN*^{IE182,183AA}. U.M. contributed to the genetic complementation analysis of KN engineered versions. G.J. initially developed this project. M.P. and G.J. analyzed and discussed the data and wrote the paper.

Received: May 20, 2011
Revised: February 1, 2012
Accepted: March 2, 2012
Published online: May 14, 2012

REFERENCES

Assaad, F.F., Huet, Y., Mayer, U., and Jürgens, G. (2001). The cytokinesis gene KEULE encodes a Sec1 protein that binds the syntaxin KNOLLE. J. Cell Biol. *152*, 531–543.

Bassham, D.C., Sanderfoot, A.A., Kovaleva, V., Zheng, H., and Raikhel, N.V. (2000). AtVPS45 complex formation at the trans-Golgi network. Mol. Biol. Cell *11*, 2251–2265.

Bracher, A., and Weissenhorn, W. (2002). Structural basis for the Golgi membrane recruitment of Sly1p by Sed5p. EMBO J. *21*, 6114–6124.

Burkhardt, P., Hattendorf, D.A., Weis, W.I., and Fasshauer, D. (2008). Munc18a controls SNARE assembly through its interaction with the syntaxin N-peptide. EMBO J. *27*, 923–933.

Carr, C.M., and Rizo, J. (2010). At the junction of SNARE and SM protein function. Curr. Opin. Cell Biol. *22*, 488–495.

Clough, S.J., and Bent, A.F. (1998). Floral dip: a simplified method for Agrobacterium-mediated transformation of Arabidopsis thaliana. Plant J. *16*, 735–743.

D'Andrea-Merrins, M., Chang, L., Lam, A.D., Ernst, S.A., and Stuenkel, E.L. (2007). Munc18c interaction with syntaxin 4 monomers and SNARE complex intermediates in GLUT4 vesicle trafficking. J. Biol. Chem. *282*, 16553–16566.

Dettmer, J., Hong-Hermesdorf, A., Stierhof, Y.D., and Schumacher, K. (2006). Vacuolar H+-ATPase activity is required for endocytic and secretory trafficking in Arabidopsis. Plant Cell *18*, 715–730.

Dhonukshe, P., Baluska, F., Schlicht, M., Hlavacka, A., Samaj, J., Friml, J., and Gadella, T.W.J., Jr. (2006). Endocytosis of cell surface material mediates cell plate formation during plant cytokinesis. Dev. Cell *10*, 137–150.

Diao, J., Su, Z., Lu, X., Yoon, T.Y., Shin, Y.K., and Ha, T. (2010). Single-vesicle fusion assay reveals Munc18-1 binding to the SNARE core is sufficient for stimulating membrane fusion. ACS Chem. Neurosci. *1*, 168–174.

Dulubova, I., Sugita, S., Hill, S., Hosaka, M., Fernandez, I., Südhof, T.C., and Rizo, J. (1999). A conformational switch in syntaxin during exocytosis: role of munc18. EMBO J. *18*, 4372–4382.

Dulubova, I., Khvotchev, M., Liu, S., Huryeva, I., Südhof, T.C., and Rizo, J. (2007). Munc18-1 binds directly to the neuronal SNARE complex. Proc. Natl. Acad. Sci. USA *104*, 2697–2702.

Geldner, N., Anders, N., Wolters, H., Keicher, J., Kornberger, W., Muller, P., Delbarre, A., Ueda, T., Nakano, A., and Jürgens, G. (2003). The Arabidopsis GNOM ARF-GEF mediates endosomal recycling, auxin transport, and auxin-dependent plant growth. Cell *112*, 219–230.

Gerber, S.H., Rah, J.C., Min, S.W., Liu, X., de Wit, H., Dulubova, I., Meyer, A.C., Rizo, J., Arancillo, M., Hammer, R.E., et al. (2008). Conformational switch of syntaxin-1 controls synaptic vesicle fusion. Science *321*, 1507–1510.

Hammarlund, M., Palfreyman, M.T., Watanabe, S., Olsen, S., and Jorgensen, E.M. (2007). Open syntaxin docks synaptic vesicles. PLoS Biol. *5*, e198.

Heese, M., Gansel, X., Sticher, L., Wick, P., Grebe, M., Granier, F., and Jürgens, G. (2001). Functional characterization of the KNOLLE-interacting t-SNARE AtSNAP33 and its role in plant cytokinesis. J. Cell Biol. *155*, 239–249.

Hu, S.H., Latham, C.F., Gee, C.L., James, D.E., and Martin, J.L. (2007). Structure of the Munc18c/Syntaxin4 N-peptide complex defines universal features of the N-peptide binding mode of Sec1/Munc18 proteins. Proc. Natl. Acad. Sci. USA *104*, 8773–8778.

Jewell, J.L., Oh, E., Bennett, S.M., Meroueh, S.O., and Thurmond, D.C. (2008). The tyrosine phosphorylation of Munc18c induces a switch in binding specificity from syntaxin 4 to Doc2beta. J. Biol. Chem. *283*, 21734–21746.

Jürgens, G. (2005). Plant cytokinesis: fission by fusion. Trends Cell Biol. *15*, 277–283.

Lauber, M.H., Waizenegger, I., Steinmann, T., Schwarz, H., Mayer, U., Hwang, I., Lukowitz, W., and Jürgens, G. (1997). The Arabidopsis KNOLLE protein is a cytokinesis-specific syntaxin. J. Cell Biol. *139*, 1485–1493.

Liu, J., Ernst, S.A., Gladycheva, S.E., Lee, Y.Y., Lentz, S.I., Ho, C.S., Li, Q., and Stuenkel, E.L. (2004). Fluorescence resonance energy transfer reports properties of syntaxin1a interaction with Munc18-1 in vivo. J. Biol. Chem. *279*, 55924–55936.

Lukowitz, W., Mayer, U., and Jürgens, G. (1996). Cytokinesis in the Arabidopsis embryo involves the syntaxin-related KNOLLE gene product. Cell *84*, 61–71.

Ma, C., Li, W., Xu, Y., and Rizo, J. (2011). Munc13 mediates the transition from the closed syntaxin-Munc18 complex to the SNARE complex. Nat. Struct. Mol. Biol. *18*, 542–549.

Margittai, M., Fasshauer, D., Jahn, R., and Langen, R. (2003a). The Habc domain and the SNARE core complex are connected by a highly flexible linker. Biochemistry *42*, 4009–4014.

Margittai, M., Widengren, J., Schweinberger, E., Schröder, G.F., Felekyan, S., Haustein, E., König, M., Fasshauer, D., Grubmüller, H., Jahn, R., and Seidel, C.A. (2003b). Single-molecule fluorescence resonance energy transfer reveals a dynamic equilibrium between closed and open conformations of syntaxin 1. Proc. Natl. Acad. Sci. USA *100*, 15516–15521.

Mayer, U., Torres Ruiz, R.A., Berleth, T., Miséra, S., and Jürgens, G. (1991). Mutations affecting body organization in the Arabidopsis embryo. Nature *353*, 402–407.

Miller, J.H. (1972). Assay of beta-galactosidase. Experiments in Molecular Biology (Cold Spring Harbor, New York: CSH Laboratory Press), pp. 352–355.

Misura, K.M.S., Scheller, R.H., and Weis, W.I. (2000). Three-dimensional structure of the neuronal-Sec1-syntaxin 1a complex. Nature *404*, 355–362.

Müller, I., Wagner, W., Völker, A., Schellmann, S., Nacry, P., Küttner, F., Schwarz-Sommer, Z., Mayer, U., and Jürgens, G. (2003). Syntaxin specificity of cytokinesis in Arabidopsis. Nat. Cell Biol. *5*, 531–534.

Nagai, T., Ibata, K., Park, E.S., Kubota, M., Mikoshiba, K., and Miyawaki, A. (2002). A variant of yellow fluorescent protein with fast and efficient maturation for cell-biological applications. Nat. Biotechnol. *20*, 87–90.

Pimpl, P., Movafeghi, A., Coughlan, S., Denecke, J., Hillmer, S., and Robinson, D.G. (2000). In situ localization and in vitro induction of plant COPI-coated vesicles. Plant Cell *12*, 2219–2236.

Rathore, S.S., Bend, E.G., Yu, H., Hammarlund, M., Jorgensen, E.M., and Shen, J. (2010). Syntaxin N-terminal peptide motif is an initiation factor for the assembly of the SNARE-Sec1/Munc18 membrane fusion complex. Proc. Natl. Acad. Sci. USA *107*, 22399–22406.

Reichardt, I., Stierhof, Y.D., Mayer, U., Richter, S., Schwarz, H., Schumacher, K., and Jürgens, G. (2007). Plant cytokinesis requires de novo secretory trafficking but not endocytosis. Curr. Biol. *17*, 2047–2053.

Reichardt, I., Slane, D., El Kasmi, F., Knöll, C., Fuchs, R., Mayer, U., Lipka, V., and Jürgens, G. (2011). Mechanisms of functional specificity among plasma-membrane syntaxins in *Arabidopsis*. Traffic *12*, 1269–1280.

Sanderfoot, A.A., Ahmed, S.U., Marty-Mazars, D., Rapoport, I., Kirchhausen, T., Marty, F., and Raikhel, N.V. (1998). A putative vacuolar cargo receptor

partially colocalizes with AtPEP12p on a prevacuolar compartment in Arabidopsis roots. Proc. Natl. Acad. Sci. USA *95*, 9920–9925.

Sanderfoot, A.A., Assaad, F.F., and Raikhel, N.V. (2000). The Arabidopsis genome. An abundance of soluble N-ethylmaleimide-sensitive factor adaptor protein receptors. Plant Physiol. *124*, 1558–1569.

Stierhof, Y.D., and El Kasmi, F. (2010). Strategies to improve the antigenicity, ultrastructure preservation and visibility of trafficking compartments in Arabidopsis tissue. Eur. J. Cell Biol. *89*, 285–297.

Südhof, T.C., and Rothman, J.E. (2009). Membrane fusion: grappling with SNARE and SM proteins. Science *323*, 474–477.

Sutton, R.B., Fasshauer, D., Jahn, R., and Brunger, A.T. (1998). Crystal structure of a SNARE complex involved in synaptic exocytosis at 2.4 A resolution. Nature *395*, 347–353.

Touihri, S., Knöll, C., Stierhof, Y.D., Müller, I., Mayer, U., and Jürgens, G. (2011). Functional anatomy of the Arabidopsis cytokinesis-specific syntaxin KNOLLE. Plant J. *68*, 755–764.

Uemura, T., Ueda, T., Ohniwa, R.L., Nakano, A., Takeyasu, K., and Sato, M.H. (2004). Systematic analysis of SNARE molecules in Arabidopsis: dissection of the post-Golgi network in plant cells. Cell Struct. Funct. *29*, 49–65.

Van Damme, D., Gadeyne, A., Vanstraelen, M., Inzé, D., Van Montagu, M.C., De Jaeger, G., Russinova, E., and Geelen, D. (2011). Adaptin-like protein TPLATE and clathrin recruitment during plant somatic cytokinesis occurs via two distinct pathways. Proc. Natl. Acad. Sci. USA *108*, 615–620.

Völker, A., Stierhof, Y.D., and Jürgens, G. (2001). Cell cycle-independent expression of the Arabidopsis cytokinesis-specific syntaxin KNOLLE results in mistargeting to the plasma membrane and is not sufficient for cytokinesis. J. Cell Sci. *114*, 3001–3012.

Waizenegger, I., Lukowitz, W., Assaad, F.F., Schwarz, H., Jürgens, G., and Mayer, U. (2000). The Arabidopsis KNOLLE and KEULE genes interact to promote vesicle fusion during cytokinesis. Curr. Biol. *10*, 1371–1374.

Weijers, D., Van Hamburg, J.P., Van Rijn, E., Hooykaas, P.J., and Offringa, R. (2003). Diphtheria toxin-mediated cell ablation reveals interregional communication during Arabidopsis seed development. Plant Physiol. *133*, 1882–1892.

Wickner, W. (2010). Membrane fusion: five lipids, four SNAREs, three chaperones, two nucleotides, and a Rab, all dancing in a ring on yeast vacuoles. Annu. Rev. Cell Dev. Biol. *26*, 115–136.

Yamaguchi, T., Dulubova, I., Min, S.W., Chen, X., Rizo, J., and Südhof, T.C. (2002). Sly1 binds to Golgi and ER syntaxins via a conserved N-terminal peptide motif. Dev. Cell *2*, 295–305.

Zouhar, J., Rojo, E., and Bassham, D.C. (2009). AtVPS45 is a positive regulator of the SYP41/SYP61/VTI12 SNARE complex involved in trafficking of vacuolar cargo. Plant Physiol. *149*, 1668–1678.